EUROPEAN JOURNAL OF CANCER 46 (2010) 198–206

available at www.sciencedirect.com

ScienceDirect

journal homepage: www.ejconline.com

Defining the optimal biological dose of NGR-hTNF, a selective vascular targeting agent, in advanced solid tumours

Vanesa Gregorc [a], Giovanni Citterio [a], Giordano Vitali [a], Anna Spreafico [a], Paola Scifo [b], Anna Borri [a], Giovanni Donadoni [a], Gilda Rossoni [a], Angelo Corti [d], Federico Caligaris-Cappio [a,f], Alessandro Del Maschio [c,f], Antonio Esposito [c], Francesco De Cobelli [c], Flavio Dell'Acqua [b], Antonella Troysi [g], Paolo Bruzzi [e], Antonio Lambiase [g], Claudio Bordignon [f,g,]*

[a] *Department of Oncology, Istituto Scientifico San Raffaele, Milan, Italy*
[b] *Department of Nuclear Medicine, Istituto Scientifico San Raffaele, Milan, Italy*
[c] *Department of Radiology, Istituto Scientifico San Raffaele, Milan, Italy*
[d] *Tumor Biology and Vascular Targeting Unit, Istituto Scientifico San Raffaele, Milan, Italy*
[e] *Clinical Epidemiology Unit, Istituto Nazionale per la Ricerca sul Cancro, Genoa, Italy*
[f] *Università Vita-Salute San Raffaele, Milan, Italy*
[g] *MolMed, Milan, Italy*

ARTICLE INFO

Article history:
Received 1 September 2009
Received in revised form 18 September 2009
Accepted 2 October 2009
Available online 10 November 2009

Keywords:
NGR-hTNF
Phase I
Solid tumours

ABSTRACT

Background: NGR-hTNF consists of human tumour necrosis factor-alpha (hTNF-α) fused to the tumour-homing peptide NGR, a ligand of an aminopeptidase N/CD13 isoform, which is overexpressed on endothelial cells of newly formed tumour blood vessels. NGR-TNF showed a biphasic dose–response curve in preclinical models. This study exploring the low-dose range aimed to define safety and optimal biological dose of NGR-hTNF.

Patients and methods: Pharmacokinetics, plasma biomarkers and dynamic contrast-enhanced magnetic resonance imaging (DCE-MRI) were evaluated at baseline and after each cycle in 16 patients enrolled at four doubling-dose levels (0.2–0.4–0.8–1.6 μg/m^2). NGR-hTNF was given intravenously as 1-h infusion every 3 weeks (q3w). Tumour response was assessed q6w.

Results: Eighty-three cycles (median, 2; range, 1–29) were administered. Most frequent treatment-related toxicity was grade 1–2 chills (69%), occurring during the first infusions. Only one patient treated at 1.6 μg/m^2 had a grade 3 drug-related toxicity (chills and dyspnoea). Both C_{max} and AUC increased proportionally with dose. No shedding of soluble TNF-α receptors was observed up to 0.8 μg/m^2. Seventy-five percent of DCE-MRI assessed patients showed a decrease over time of K^{trans}, which was more pronounced at 0.8 μg/m^2. Seven patients (44%) had stable disease for a median time of 5.9 months, including a colon cancer patient who experienced an 18-month progression-free time.

Conclusion: Based on tolerability, soluble TNF-receptors kinetics, anti-vascular effect and disease control, NGR-hTNF 0.8 μg/m^2 will be further developed either as single-agent or with standard chemotherapy.

* *Corresponding author:* Address: Via Olgettina, 58, 20132 Milan, Italy. Tel.: +39 02 2643 2351; fax: +39 02 2643 2285.
E-mail address: claudio.bordignon@hsr.it (C. Bordignon).
0959-8049/$ - see front matter
doi:10.1016/j.ejca.2009.10.005

1. Introduction

TNF-α was originally identified for its potent cytotoxic activity against different tumour cell lines and for its ability to induce apoptosis of tumour-associated endothelial cells and massive haemorrhagic necrosis of transplanted tumours.[1,2] However, the early-stage clinical development of TNF-α was hampered by its severe systemic toxicity, the maximum-tolerated dose (MTD) being significantly lower than the effective dose in preclinical models.[3–8] More recently, isolated limb perfusion employing very high doses of TNF-α in combination with chemotherapy induced elevated complete response rates in patients with melanoma[2] or sarcoma[9] of the extremities, as well as the regression of bulky hepatic cancers[10] confined to the liver. The anti-vascular effects of TNF-α provided the rationale for developing a vascular targeting strategy aimed at increasing the local antitumour activity and at enabling systemic administration of therapeutic doses.

NGR-hTNF is a selective vascular targeting agent (VTA) that has been prepared by fusing the N-terminus of recombinant human TNF-α with the C-terminus of the tumour-homing asparagine-glycine-arginine (NGR)-peptide, a ligand of a CD13 (aminopeptidase N) form overexpressed by endothelial cells of newly formed tumour blood vessels.[11–14] CD13 is a membrane-bound metalloprotease thought to play a role in chemokine processing, tumour invasion and angiogenesis.[11–13] In preclinical models, murine NGR-TNF showed a biphasic dose–response curve with antitumour activity observed even at doses in the picogram range (100 pg/mouse),[11,15] equivalent in humans to a dose of 0.2 μg/m^2, the selected starting dose of the phase I trial.

Two phase I trials were designed for NGR-hTNF. A dose-escalation study evaluating a wide dose-interval from 0.2 to 60 μg/m^2, established the MTD at 45 μg/m^2 once every 3 weeks, with dose-limiting toxicities being characterised by grade 3 dyspnoea and acute infusion reaction.[16] The present phase I trial was undertaken to further explore the low-dose range from 0.2 to 1.6 μg/m^2 and select the optimal biological dose of NGR-hTNF for phase II development.

2. Patients and methods

2.1. Eligibility criteria

Key inclusion criteria were aged 18 years or older; advanced solid tumours refractory to standard treatments; Eastern Cooperative Oncology Group performance status $\leqslant 2$. Patients with significant cardiac, hepatic, renal dysfunction or cerebral metastases, as well as patients completing radiation therapy or systemic therapy within 4 weeks or having surgery within 2 weeks before treatment start were excluded. All patients gave written informed consent before any study-related procedure was performed. The protocol was approved by local Ethical Committee.

2.2. Study design and dosing

This was a single-centre, single-agent, phase I study with four patients to be enrolled at each of four planned low-dose levels. Primary objective was to define the safety profile of low doses of NGR-hTNF. Secondary aims included pharmacokinetic, pharmacodynamic and antitumour activity assessments. NGR-hTNF was administered intravenously as 60-min infusion every 3 weeks at the starting dose of 0.2 μg/m^2 followed by a doubling-dose scheme (0.4–0.8–1.6 μg/m^2). Before the infusion, NGR-hTNF in phosphate buffered saline was diluted to the appropriate concentration with 0.9% sodium chloride containing human serum albumin (HSA).

2.3. Definition of DLT

Dose-limiting toxicity (DLT) applicable to the study was defined as any first-cycle treatment-related grade 4 haematologic or grades 3–4 non-haematologic toxicity with the exclusion of nausea, vomiting and fever that could be rapidly controlled with supportive care. At each dose level, the first patient had to complete one cycle before subsequent patients were allowed to be included. In order to fully document the safety profile, a cohort expansion up to six patients was planned in the presence of DLT.

2.4. Tumour response and safety

Tumour measurements were done within 14 days before study treatment start, and thereafter every other cycle (6 weeks) until progressive disease, or unacceptable toxicity. Measurable target lesions were evaluated for response using the Response Evaluation Criteria in Solid Tumours (RECIST) and the duration of stable disease was measured from treatment start until criteria for progression were met. Patient history, physical examination and laboratory analyses were assessed at baseline and before each treatment course. Adverse events were recorded from the first day of treatment to 28 days after last dose and were graded according to the Common Terminology Criteria for Adverse Events (CTC-AE), version 3.0.

2.5. Pharmacokinetics and exploratory analysis of biological markers

Intensive pharmacokinetic (PK) blood sampling was performed on the first day of study treatment with samples drawn before infusion and six time-points up to 4 h after each infusion (at 5, 15, 30, 60, 120 and 240 min). NGR-hTNF concentrations were computed using an enzyme-linked immunosorbent assay (ELISA). Pharmacokinetic parameters, including maximum plasma concentration (C_{max}) and area under the plasma concentration–time curve up to the last detectable concentration (AUC), were estimated using the standard non-compartmental methods. Plasma samples were also tested for detecting anti-NGR-hTNF antibodies and monitoring circulating levels of soluble TNF receptors (sTNF-RI and sTNF-RII), by a quantitative sandwich enzyme immunoassay technique. Chromogranin A (CgA) plasma levels were measured by using a sandwich ELISA system between a monoclonal anti-CgA antibody (mAb B4E11), chromogranin A and a rabbit-polyclonal anti-CgA antiserum. Blood samples were also evaluated for monitoring circulating endothelial cells (CECs) (prior to, 4 and 24 h after infusion) and circulating tumour cells

(CTCs) analysis (prior to and 24 h after infusion). In order to select biomarkers potentially modified by study treatment, samples from 15 patients, collected at 0–120–240 min after starting of the first infusion, were sent to a specialised company (Rules Based Medicine Inc., Austin, TX) for Multi-Analyte Profile (MAP) testing, a screening analysis in which up to 90 biomarkers are simultaneously evaluated on each sample.

2.6. Dynamic contrast-enhanced magnetic resonance imaging (DCE-MRI)

Magnetic resonance imaging studies were performed on a 1.5T MR scanner (Philips Medical System, Best, The Netherlands). At each scanning session, standard T1- and T2-weighted images were first obtained to assess disease and locate lesions. In order to calculate gadopentetate dimeglumine (Gd-DPTA) concentration, proton density-weighted three-dimensional (3D) images were first acquired.[17] Then, a dynamic series of 45 T1-weighted 3D images (10 slices with temporal resolution of 2 s) were acquired on the same slice locations with a simultaneous automatic injection of 0.1 mmol/Kg Gd-DTPA (Magnevist, Schering AG, Berlin, Germany) at a flow rate of 2 mL/s. DCE-MRI scanning was performed at baseline (48 h before the first treatment cycle) and 2 h after the administration of first and subsequent cycles. Data were analysed with a home-made software developed with MATLAB (The MathWorks Inc., Natick, MA). For each pixel, Gd-DTPA concentration curve was fitted with the standardised Tofts pharmacokinetic model,[18] and maps of K^{trans} (transfer constant from plasma to extravascular extracellular space of the tumour – EES)[19] were estimated. It has to be reminded that the transfer constant K^{trans} has several physiologic interpretations, depending on the balance between capillary permeability and blood flow in the tissue of interest. In high-permeability situations (where tracer flux is flow limited), the transfer constant is equal to the blood plasma flow per unit volume of tissue. In the other limiting case of low permeability, where tracer flux is limited by the permeability, the transfer constant is equal to the permeability surface area product between blood plasma and the EES, per unit volume of tissue. Thus, a reduction of K^{trans} would mean either a reduction of the amount of capillaries or a reduction of permeability, or both situations. The arterial input function (AIF) used in the kinetic model was calculated on a major artery close to the site of the tumour for each session of each patient. The initial area under the concentration–time curve over 60 s post-contrast arrival in the tissue (IAUGC) as a semi-quantitative index was also obtained. Regions of interest (ROIs) were drawn by expert radiologist in the tumour mass. ROIs were accurately traced in order to include the areas of tumour tissue with intense enhancement in the baseline DCE-MRI study avoiding the inclusion of tumour areas with necrotic appearance at MRI. During the DCE-MRI studies performed after each cycle, ROIs were drawn just alike in the baseline study.

2.7. Data analysis

Descriptive statistics were provided for all end-points presented. All continuous measurements were summarised by mean (plus or minus standard deviation) or median (with ranges) for non-normal data and by frequency counts and percentages for categorical data. For DCE-MRI parameters, the change from baseline (expressed as percentage) was reported and to determine if the distribution of these changes differed significantly from zero, a Wilcoxon signed-rank test was used. Progression-free survival, computed from baseline until disease progression or death, and overall survival, calculated from baseline until death, were estimated using the Kaplan–Meier method. This trial is registered with ClinicalTrial.gov, number NCT00419328.

3. Results

3.1. Patients

Sixteen patients were enrolled between March 2005 and March 2006. Patient demographics, baseline characteristics and prior therapies are listed in Table 1.

3.2. Safety

Eighty-three cycles of therapy were administered (mean, 5.2; median, 2; range, 1–29) and five patients (31%) received 6

Table 1 – Demographics, baseline characteristics and prior treatments.

Characteristics	No. of patients, $n = 16$ (%)
Sex	
Male	10 (63)
Female	6 (37)
Age, years	
Median (range)	60 (43-73)
ECOG performance status	
0	5 (31)
1	10 (63)
2	1 (6)
Primary tumour type	
Colorectal	6 (37)
Renal	3 (19)
Liver	2 (13)
NSCLC	2 (13)
Carcinoid	1 (6)
Pancreatic	1 (6)
Gastric	1 (6)
Prior therapy	
Chemotherapy	16 (100)
Surgery	14 (88)
Radiation therapy	7 (44)
Hormone therapy	3 (19)
Immunotherapy	2 (13)
Number of prior therapy lines	
Median (range)	4 (1–8)
1 line	16 (100)
2 lines	12 (75)
3 lines	10 (63)
$\geqslant$4 lines	7 (44)

Abbreviations: ECOG, Eastern Cooperative Oncology Group; NSCLC, non-small cell lung cancer.

Table 2 – Treatment-emergent adverse events (worst grade per patient), occurring in ⩾20% of patients or reaching grade 3 intensity.

Adverse event	All grades, *n* (%)	Grade 1, *n* (%)	Grade 2, *n* (%)	Grade 3, *n* (%)	Grade 4, *n* (%)
Chills	11 (69)	6 (38)	4 (25)	1 (6)	–
Anaemia	7 (44)	–	6 (38)	1 (6)	–
Pain	7 (44)	1 (6)	6 (38)	–	–
Asthenia	7 (44)	4 (25)	3 (19)	–	–
BP increase	7 (44)	5 (31)	2 (13)	–	–
Fever	5 (31)	4 (25)	1 (6)	–	–
Nausea	3 (19)	1 (6)	2 (13)	–	–
Vomiting	3 (19)	2 (13)	1 (6)	–	–
Oedema	3 (19)	3 (19)	–	–	–
Pleural effusion	2 (13)	–	–	2 (13)	-
Dyspnoea	2 (13)	–	–	2 (13)	–
Diarrhoea	2 (13)	–	1 (6)	1 (6)	–
Anorexia	1 (6)	–	–	1 (6)	–
Parotitis	1 (6)	–	–	1 (6)	–
Proctorrhagia	1 (6)	–	–	1 (6)	–
Melaena	1 (6)	–	–	1 (6)	–
Pyelonephritis	1 (6)	–	–	1 (6)	–
Cardiac ischaemia	1 (6)	–	–	1 (6)	–
GGT increase	1 (6)	–	–	1 (6)	–
AST increase	1 (6)	–	–	1 (6)	–

Abbreviations: BP, blood pressure; GGT, gamma-glutamyl transpeptidase; AST, aspartate transaminase. Nine patients experienced 15 grade 3 events; 1 patient had 5 grade 3 toxicities (diarrhoea, anorexia, parotitis, proctorrhagia and melaena).

doses or more. NGR-hTNF was well tolerated across planned dose levels and neither grade 4 adverse events nor treatment-related deaths were reported. Thirteen patients (81%) were withdrawn for progressive disease and two patients (13%) discontinued therapy for grade 3 adverse events after the first cycle (an asymptomatic cardiac ischaemia and chills with dyspnoea). One patient (6%) remains on study after a follow-up of 3.6 years.

Overall, 121 treatment-emergent adverse events were registered those occurring in ⩾20% of patients or reaching grade 3 in severity are listed in Table 2.

Only 27 adverse events (22%) were considered treatment related (Table 3) and the most frequent were chills, registered over 12 cycles (14%), and transient blood pressure increase, reported for 9 cycles (11%). Median time-to-onset and duration of these treatment-related adverse events were 34 min (range, 14–80 min) and 20 min (range, 14–40 min), respectively. Chills promptly resolved without (55%) or with (45%) appropriate treatment (i.e. acetaminophen/paracetamol). No therapy was administered for managing the transient blood pressure increases. One patient treated at 1.6 μg/m^2 had grade 3 chills and dyspnoea, defined as DLT. However, considering that 1.6 μg/m^2 was the highest dose level planned to be explored and that MTD was determined at 45 μg/m^2 in another trial, there was no further expansion of this cohort.

3.3. *Pharmacokinetics and biologic markers*

Concentration–time profiles for each patient were adjusted for baseline levels by subtracting the time-zero value to all other time-point values, due to background levels of TNF-α generally detectable in cancer patients. Following the first course, both C_{max} and AUC increased proportionally with dose ($r^2 = 0.98$, $p < .001$ and $r^2 = 0.96$, $p < .02$, respectively) (Fig. 1A and B). Mean (±SD) C_{max} at 0.2 (given as 20-min infusion), 0.4, 0.8 and 1.6 μg/m^2 were 4.69 (±0.47), 5.83 (±1.62), 9.05 (±4.88) and 19.4 (±4.30) pg/mL, respectively. The apparent elimination half-life ($t_{1/2}$) was relatively short, with means ranging from 0.60 (±0.04) to 1.35 (±0.97) h. Time-to-peak plasma concentration (t_{max}) was reached in the range of 30–60 min and low concentrations were detectable up to 4 h post-dose. Average systemic exposure to NGR-hTNF on cycles 2 and 3 was comparable to that found on cycle 1 (data not shown).

Due to an extremely high variability of baseline levels of soluble TNF receptors (sTNF-RI and sTNF-RII), values obtained at different time-points after each cycle were normalised by subtracting the time-zero value. At 0.2, 0.4 and 0.8 μg/m^2, the levels of both circulating receptors were scattered around zero, indicating no stimulation by NGR-hTNF. Increase of the concentrations of both receptors was only noted at 1.6 μg/m^2 (Fig. 1C and D). This effect was twofold higher for sTNF-RII than for sTNF-RI and occurred approximately 30 min after maximal NGR-hTNF concentration.

None of the 15 patients evaluated for the detection of anti-NGR-hTNF showed circulating antibodies during treatment.

No correlations between study treatment and both circulating endothelial cells (CECs) and circulating tumour cells were detected. However, in this analysis CECs were not segregated based on whether or not they were viable.

NGR-hTNF induced only minor changes in chromogranin A (CgA) levels ranging from 95% of baseline-value after 1 h to 105% of baseline-value after 4 h. Nevertheless, the difference between CgA levels at these two time-points was statistically significant ($p = .004$; two-tailed *t* test, paired), suggesting that NGR-hTNF can induce rapid changes in CgA levels, possibly by affecting its clearance or its secretion by the neuroendocrine system.

Table 3 – Treatment-related adverse events by dose levels.

	Dose levels											
	0.2 μg/m^2 (n = 4)			0.4 μg/m^2 (n = 4)			0.8 μg/m^2 (n = 4)			1.6 μg/m^2 (n = 4)		
Toxicity (grade)	1	2	3	1	2	3	1	2	3	1	2	3
Chills	1	–	–	2	–	–	3	1	–	–	3	1
BP increase	–	–	–	1	–	–	3	–	–	1	2	–
Dyspnoea	–	–	–	–	–	–	–	–	–	–	–	1
Asthenia	1	–	–	–	–	–	–	–	–	–	–	–
Fever	–	1	–	–	–	–	–	–	–	–	–	–
Tachycardia	1	–	–	–	–	–	–	–	–	–	–	–
Arthralgia	1	–	–	–	–	–	–	–	–	–	–	–
Vomiting	–	–	–	1	–	–	–	–	–	–	–	–

Abbreviations: BP, blood pressure.

Screening analysis identified some analytes, especially macrophage inflammatory protein-1 beta (MIP-1β), for which a low inter-patient variability in baseline levels was noted, ranging from 101 to 249 pg/ml. Across all dose levels, a relative increase at 2 h versus baseline was observed, and this increase (fourfold) was statistically significant at 0.8 μg/m^2 and particularly relevant (20-fold) at 1.6 μg/m^2 (p = .005 and p = .1, respectively; two-tailed t test, paired).

3.4. *Dynamic imaging*

The relationship of NGR-hTNF dose and anti-vascular effect was evaluated in 12 patients by DCE-MRI. Following the first cycle, the median changes in K^{trans} within the regions of interest (ROIs) were +4% (p = .7, Wilcoxon signed-rank test), +13% (p = .04; 95% confidence interval (CI), –7% to +52%), –17% (p = .02; 95% CI, –23% to +3%), and +13% (p = .1) in the 0.2 (n = 3 patients, 10 ROIs), 0.4 (n = 3, 9 ROIs), 0.8 (n = 4, 15 ROIs) and 1.6 μg/m^2 (n = 2, 4 ROIs) dose cohorts, respectively.

Maximal changes in K^{trans} within the ROIs by dose levels are shown in Fig. 2A. A statistically significant reduction was observed when all ROIs from the four dose cohorts were analysed together (median, –24%; 95% CI, –37% to –17%; p = .01). The median K^{trans} values in the 0.2, 0.4, 0.8 and 1.6 μg/m^2 dose groups corresponded to relative changes of –27% (p = .2), –18% (p = .8), –37% (p = .0001; 95% CI, –55% to –23%) and +17% (p = .6), respectively.

Changes in K^{trans} over time, averaged for each patient across all his or her ROIs, for the twelve evaluated patients are shown in Fig. 2B. Overall, 9 patients (75%) showed a decrease at some point during treatment (median, –15%; 95% CI, –32% to 4.5%; p = .03). Similar results were also noted for the IAUGC (data not shown).

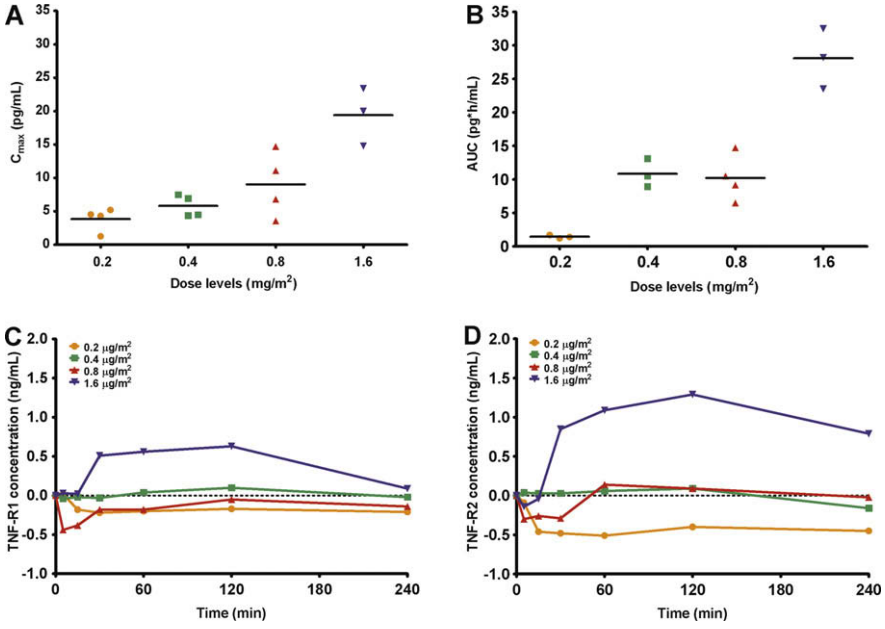

Fig. 1 – Individual and mean C_{max} (A) and AUC (B) following the first cycle of NGR-hTNF by dose levels. Mean plasma concentrations of soluble receptors TNF-RI (C) and sTNF-RII (D) during the first cycle of NGR-hTNF by dose levels. *Abbreviations*: C_{max}, maximum plasma concentration; AUC, area under the plasma concentration–time curve up to the last detectable concentration. *Footnotes*: Symbols, individual measurements; short solid lines, mean values. All values were adjusted for baseline levels by subtracting the time-zero value to all other time-points values.

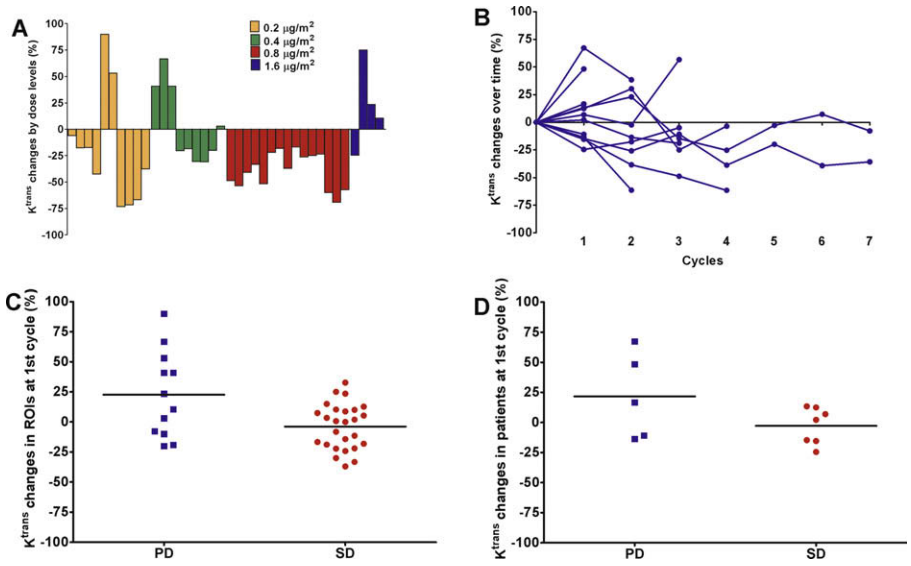

Fig. 2 – Maximal changes in K^{trans} from baseline within the regions of interest (ROIs) by dose level (A). K^{trans} changes in patients over time (B). ROI (C) and patient (D) changes in K^{trans} after the first cycle by status at first tumour restaging. *Abbreviations*: DCE-MRI, dynamic contrast-enhanced magnetic resonance imaging; K^{trans}, transfer constant from plasma to extravascular extracellular space; PD, progressive disease; SD, stable disease. Symbols, individual measurements; short solid lines, mean values. *Footnotes*: Twelve patients were assessed by DCE-MRI out of 16 enrolled. Two cases were excluded for MRI artefacts and two for necrosis and lung collapse, respectively. Data (expressed as percentage) are reported in figure A as maximal change from baseline registered at any time in each region of interest (ROIs), in figure B as change in patients over time, in figure C as change in ROIs at first cycle and in figure D as change in patients at first cycle for patients who had progressive disease (PD) or stable disease (SD) at first postbaseline assessment after 2 cycles. Analysis of the K^{trans} differences between post- and pre-treatment values was performed using the Wilcoxon signed-rank test. Analysis of the K^{trans} differences at first cycle between patients with SD or PD after the second cycle was performed using the Mann–Whitney test.

Table 4 – Characteristics of patients with stable disease.

DL	Pt. No.	Gender/age (yrs)	Primary tumor	Metastatic sites	No. of prior regimens	Best response to prior regimen/time to progression (months)	Dose ($\mu g/m^2$)	No. of cycles	Duration of SD (months)
1	1	F/61	Colon	Liver, peritoneal carcinosis	8	PD/2	0.2	3	2.4
	3	F/43	Colon	Abdomen	3	PD/3	0.2 (0.8)	9 (20)	17.8
2	9	F/43	Carcinoid	Liver	4	SD/9	0.4	10	8.2
3	6	M/56	Renal	Lung, liver, nodes, adrenal gland	4	NE/4	0.8	8	5.9
	11	M/68	Liver	Adrenal gland, nodes	2	PD/1	0.8	4	2.9
	12	M/70	Renal	Lung, nodes	5	PD/1	0.8	6	5.8
4	14	F/70	NSCLC	Lung	2	PR/31	1.6	9	7.5

Abbreviations: DL, dose level; Pt. No., patient number; M, male; F, female; yrs, years; PD, progressive disease; SD, stable disease; PR, partial response; NE, not evaluable; NSCLC, non-small cell lung cancer.
Footnotes: Patient number 3 was treated with 0.2 $\mu g/m^2$ for 9 cycles, followed by 20 cycles given at 0.8 $\mu g/m^2$. In patients who had SD, the median time to progression on the immediate prior regimen administered and the median duration of SD on the current study treatment were 3 and 5.9 months, respectively, with a relative growth modulation index of 1.9.

When the changes in K^{trans} at first cycle were compared in ROIs from patients classified after the second cycle as clinical non-progressors or progressors, a statistically significant difference was observed (mean ± SEM, –3.8% ± 3.7 versus +22.6% ± 10.3, $p = .03$; Mann–Whitney test) (Fig. 2C). A similar, though not statistically significant, difference was detected between the average K^{trans} changes in patients with stable or progressive disease after the second

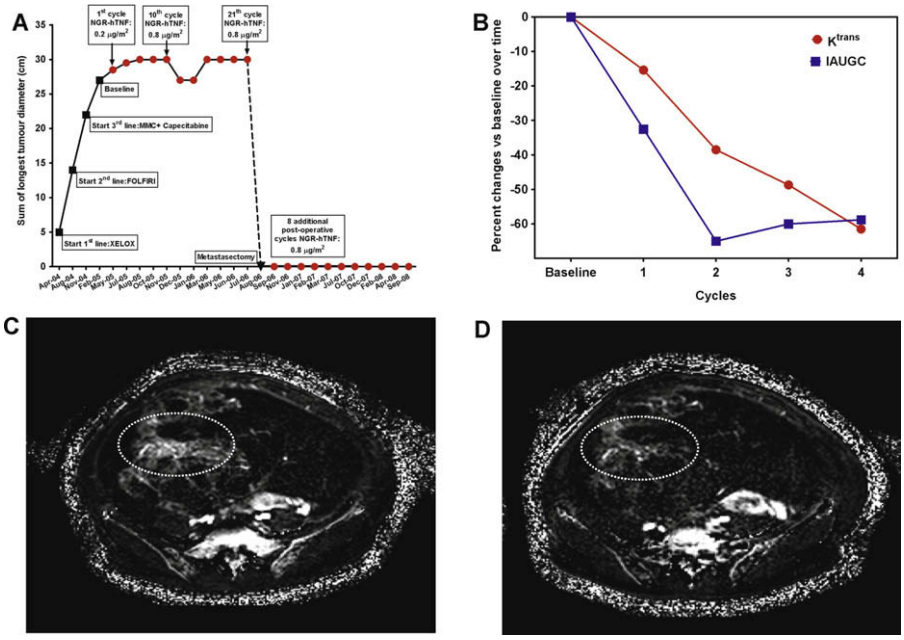

Fig. 3 – Treatment history (A) and changes in DCE-MRI (B) of a chemo-refractory colon cancer patient experiencing an 18-month stable disease. Dynamic contrast-enhanced image of the 30-cm abdominal metastasis of this patient is shown at baseline (C) and after 4 cycles (D). Abbreviations: XELOX, capecitabine, oxaliplatin; FOLFIRI, fluorouracil, leucovorin, irinotecan; MMC, mitomycin C; K^{trans}, transfer constant from plasma to extravascular extracellular space; IAUGC, initial area under the concentration–time curve over 60 s post-contrast arrival in the tissue; DCE-MRI, dynamic contrast-enhanced magnetic resonance imaging. Footnotes: The sum of longest tumour diameter over time in a colon cancer patient is shown in figure A and the percentage change from baseline of K^{trans} and IAUGC during the first 4 cycles is depicted quantitatively in figure B. This patient experienced a 59% decrease in tumour IAUGC that is mapped with an oval-shaped dotted line over the tumour region at baseline (figure C) and after the 4th cycle (figure D).

cycle (mean ± SEM, –2.8% ± 5.7 versus +21.6% ± 15.9, $p = .1$) (Fig. 2D).

3.5. *Antitumour activity*

According to an intent-to-treat analysis, seven patients (44%) had stable disease (SD) as best response for a median duration of 5.9 months (range, 2.4–17.8 months) (Table 4). Notably, a prolonged progression-free interval was observed in a 43-year-old female patient with metastatic colon cancer previously treated with three chemotherapy regimens delivered in less than 1 year. She experienced an 18-month stable disease during treatment with NGR-hTNF given at 0.2 μg/m^2 for 9 cycles, followed by 12 cycles increased at 0.8 μg/m^2. A progressive decrease of K^{trans} (median, –44%; range, –15% to –61%) and IAUGC (median, –59%; range, –32% to –65%) was noted on DCE-MRI throughout the first four cycles. Following 21 courses she successfully underwent radical metastasectomy of a 30-cm large abdominal (ovarian) mass. Her progression-free survival was censored at the time of surgery, but after a follow-up of 3.6 years the patient remained in a disease-free state following an additional eight post-operative cycles given at 0.8 μg/m^2. Fig. 3A–D shows the treatment history and the changes in DCE-MRI of this patient. Median and 6-month progression-free survival were 3.4 months and 29%, respectively. With a median follow-up time of 25.8 months (range, 2.0–43.8 months), two patients (13%) were still alive and median overall survival was 6.9 months. Median survival time among the patients with SD as the best response was 10.3 months and among those without SD was 5.5 months.

4. Discussion

The historical approach to treating advanced cancer has been to administer maximum-tolerated doses of cytotoxic chemotherapy to directly kill dividing tumour cells. In contrast to this approach, strategies using novel agents that target vascular endothelial functional integrity or endothelial cell survival pathways can result in the use of low-dose agents that may actually have more pronounced anti-vascular or antiangiogenic effects than cytotoxic effects.[20] However, the early-stage clinical development of these biological agents can be challenging.[21,22] This is compounded by the fact that the maximal antitumour activity may not necessarily coincide only with the maximum-tolerated dose, but also with a lower drug dose, i.e. the optimal biological dose. However, validated molecular, cellular or functional imaging surrogate markers of anti-vascular activity, needed to finely assess the dose–response relationship for these agents, are still lacking.[22] As a consequence, standard markers of antitumour activity such as objective tumour response and time to progression, with their well-known limitations especially in the assessment of antiangiogenic agents, are to be relied upon.

Vascular targeting agents cause direct damage to the already established tumour endothelium. There are potential advantages of these agents over other classes of anti-cancer

drug.[23] A significant bystander effect may take place, as single blood vessel may provide oxygen and nutrients for thousands of tumour cells. The endothelial cell itself does not need to be killed by the VTA, a change of structure or local initiation of the coagulation cascade may be all that is needed.

Since its discovery,[1] TNF-α has been shown to have potent anti-vascular effects in tumours, even though this cytokine unselectively binds to tumour blood vessels. Therefore, very high doses were explored in order to reproduce these therapeutic effects. Disappointingly, early clinical trials using TNF-α led to serious toxicities when used systemically at MTD.[3–8,24,25] Aiming to exploit a ligand-direct approach, human TNF-α has been genetically fused to the peptide NGR, which is able to selectively bind the tumour vasculature of several tumour types.[14]

The results of the current trial, undertaken to further explore the low-dose range of NGR-hTNF, confirmed the safe profile already characterised in the dose-escalation trial,[16] and suggest that targeted delivery of TNF-α to the tumour vasculature could significantly improve its therapeutic index. Noteworthy, the toxicity pattern was limited to short-lived chills, generally occurring during the first infusions.

A further objective of the present study was to evaluate the biological effects of the study drug. For instance, both receptors for TNF-α exist also in soluble forms, probably derived by proteolytic cleavage from the cell-surface forms.[26] Interestingly, the amount and speed of receptor shedding appear to be linearly correlated with the serum TNF-α levels.[26] These circulating receptors can compete for TNF-α with the cell-surface receptors and thus block its bioavailability and activity, serving as physiological attenuators of the TNF-α activity. In our study, shedding of circulating TNF-α receptors was observed only at the dose of 1.6 $\mu g/m^2$.

Additionally, significant increases of some other biological markers, including chromogranin A and macrophage inflammatory protein-1 beta, were noted during treatment period. Even though the clinical significance of drug-induced changes in these plasma biomarkers remains to be fully elucidated, these effects however could be suggestive of the biologic activity of NGR-hTNF and could be exploited as possible approach to monitor drug activity or to select patients for a more tailored therapy.

Tumour vascular changes during NGR-hTNF treatment were intensively monitored by dynamic imaging. It has not yet been clearly established which degree of change in K^{trans} is likely to represent a true difference due to drug effect.[27] Moreover, DCE-MRI data analysis is complex since K^{trans} values might be influenced by either the position of selected regions of interest or the definition of the arterial input function in the kinetic model. Nevertheless, it is interesting to note that NGR-hTNF at low doses appeared to have direct global effects on tumour vascular permeability and blood flow. The decrease in vascularity was more pronounced in patients receiving at least four cycles, implying that the overall effect tends to occur in the later course of therapy, and was statistically significant for the cohort treated with 0.8 $\mu g/m^2$, both after the first cycle and as maximal change over time.

Finally, the proportion of patients (44%) experiencing stabilization of disease for a median time of 5.9 months in this study appears to be clinically relevant in this heavily pre-treated patient population also considering the easily manageable toxicity profile.

Taken together, these preliminary observations on plasma biomarkers, dynamic imaging and disease control support the hypothesis that NGR-hTNF is biologically and clinically active even when administered at low doses.

The dose level of 0.8 $\mu g/m^2$ has been selected for further phase II development based on the slightly more favourable toxicity profile, with the absence of grade 3 toxicity, the promising disease control, with three stable diseases lasting for 3–6 months, the lack of stimulation of TNF-receptors shedding and the significant anti-vascular effect observed by DCE-MRI. NGR-hTNF is currently developed either as single-agent or in combination with chemotherapy.

Conflict of interest statement

None declared.

Acknowledgement

This trial was sponsored by MolMed, Milan, Italy.

REFERENCES

1. Carswell EA, Old LJ, Kassel RL, et al. An endotoxin-induced serum factor that causes necrosis of tumours. *Proc Natl Acad Sci USA* 1975;**72**:3666–70.
2. Lejeune FJ, Lienard D, Matter M, et al. Efficiency of recombinant human TNF in human cancer therapy. *Cancer Immun* 2006;**6**:6.
3. Creaven PJ, Brenner DE, Cowens JW, et al. A phase I clinical trial of recombinant human tumour necrosis factor given daily for five days. *Cancer Chemother Pharmacol* 1989;**23**:186–91.
4. Gamm H, Lindemann A, Mertelsmann R, et al. Phase I trial of recombinant human tumour necrosis factor alpha in patients with advanced malignancy. *Eur J Cancer* 1991;**27**:856–63.
5. Kimura K, Taguchi T, Urushizaki I, et al. Phase I study of recombinant human tumour necrosis factor. *Cancer Chemother Pharmacol* 1987;**20**:223–9.
6. Mittelman A, Puccio C, Gafney E, et al. A phase I pharmacokinetic study of recombinant human tumour necrosis factor administered by a 5-day continuous infusion. *Invest New Drugs* 1992;**10**:183–90.
7. Schwartz JE, Scuderi P, Wiggins C, et al. A phase I trial of recombinant tumour necrosis factor (rTNF) administered by continuous intravenous infusion in patients with disseminated malignancy. *Biotherapy* 1989;**1**:207–14.
8. Wiedenmann B, Reichardt P, Rath U, et al. Phase-I trial of intravenous continuous infusion of tumour necrosis factor in advanced metastatic carcinomas. *J Cancer Res Clin Oncol* 1989;**115**:189–92.
9. Eggermont AM, Schraffordt Koops H, Lienard D, et al. Isolated limb perfusion with high-dose tumour necrosis factor-alpha in combination with interferon-gamma and melphalan for nonresectable extremity soft tissue sarcomas: a multicenter trial. *J Clin Oncol* 1996;**14**:2653–65.
10. Alexander HR, Brown CK, Bartlett DL, et al. Augmented capillary leak during isolated hepatic perfusion (IHP) occurs

via tumour necrosis factor-independent mechanisms. *Clin Cancer Res* 1998;**4**:2357–62.
11. Curnis F, Sacchi A, Borgna L, et al. Enhancement of tumor necrosis factor alpha antitumour immunotherapeutic properties by targeted delivery to aminopeptidase N (CD13). *Nat Biotechnol* 2000;**18**:1185–90.
12. Corti A, Ponzoni M. Tumour vascular targeting with tumour necrosis factor alpha and chemotherapeutic drugs. *Ann NY Acad Sci* 2004;**1028**:104–12.
13. Colombo G, Curnis F, De Mori GM, et al. Structure-activity relationships of linear and cyclic peptides containing the NGR tumor-homing motif. *J Biol Chem* 2002;**277**:47891–7.
14. Curnis F, Arrigoni G, Sacchi A, et al. Differential binding of drugs containing the NGR motif to CD13 isoforms in tumour vessels, epithelia, and myeloid cells. *Cancer Res* 2002;**62**:867–74.
15. Curnis F, Sacchi A, Corti A. Improving chemotherapeutic drug penetration in tumours by vascular targeting and barrier alteration. *J Clin Invest* 2002;**110**:475–82.
16. van Laarhoven H, Fiedler W, Desar I, et al. Phase I and DCE-MRI evaluation of NGR-TNF, a novel vascular targeting agent, in patients with solid tumours (EORTC 16041). *J Clin Oncol* 2008;**26**:158s [abstr. 3521].
17. Parker GJ, Suckling J, Tanner SF, et al. Probing tumor microvascularity by measurement, analysis and display of contrast agent uptake kinetics. *J Magn Reson Imaging* 1997;**7**:564–74.
18. Tofts PS, Brix G, Buckley DL, et al. Estimating kinetic parameters from dynamic contrast-enhanced T(1)-weighted MRI of a diffusable tracer: standardized quantities and symbols. *J Magn Reson Imaging* 1999;**10**:223–32.
19. Collins DJ, Padhani AR. Dynamic magnetic resonance imaging of tumour perfusion. Approaches and biomedical challenges. *IEEE Eng Med Biol Mag* 2004;**23**:65–83.
20. Cooney MM, van Heeckeren W, Bhakta S, et al. Drug insight: vascular disrupting agents and angiogenesis–novel approaches for drug delivery. *Nat Clin Pract Oncol* 2006;**3**:682–92.
21. Cristofanilli M, Charnsangavej C, Hortobagyi GN. Angiogenesis modulation in cancer research: novel clinical approaches. *Nat Rev Drug Discov* 2002;**1**:415–26.
22. Bocci G, Man S, Green SK, et al. Increased plasma vascular endothelial growth factor (VEGF) as a surrogate marker for optimal therapeutic dosing of VEGF receptor-2 monoclonal antibodies. *Cancer Res* 2004;**64**:6616–25.
23. Gaya AM, Rustin GJ. Vascular disrupting agents: a new class of drug in cancer therapy. *Clin Oncol (R Coll Radiol)* 2005;**17**:277–90.
24. Fraker DL, Alexander HR, Pass HI. Biologic therapy with TNF: systemic administration and isolation-perfusion. In: De Vita V, Hellman S, Rosenberg S, editors. *Biologic therapy of cancer: principles and practice*. Philadelphia, Pennsylvania: JB Lippincott Co.; 1995. p. 329–45.
25. Lienard D, Eggermont AM, Schraffordt Koops H, et al. Isolated perfusion of the limb with high-dose tumour necrosis factor-alpha (TNF-alpha), interferon-gamma (IFN-gamma) and melphalan for melanoma stage III. Results of a multi-centre pilot study. *Melanoma Res* 1994;**4**(Suppl. 1):21–6.
26. Aderka D, Sorkine P, Abu-Abid S, et al. Shedding kinetics of soluble tumor necrosis factor (TNF) receptors after systemic TNF leaking during isolated limb perfusion. *J Clin Invest* 1998;**101**:650–9.
27. Jackson A, O'Connor JPB, Parker GJM, et al. Imaging tumour vascular heterogeneity and angiogenesis using dynamic contrast-enhanced magnetic resonance imaging. *Clin Cancer Res* 2007;**13**(12):3449–59.